

# Cooperative Computation and Communication for Mobile Edge Computing

Xiaowen Cao, *Student Member, IEEE*, Feng Wang, *Member, IEEE*, Jie Xu, *Member, IEEE*,  
Rui Zhang, *Fellow, IEEE*, and Shuguang Cui, *Fellow, IEEE*

**Abstract**—This paper proposes a novel *user cooperation* approach in both computation and communication for mobile edge computing (MEC) systems to improve the energy efficiency for latency-constrained computation. We consider a basic three-node MEC system consisting of a user node, a helper node, and an access point (AP) node attached with an MEC server, in which the user has latency-constrained and computation-intensive tasks to be executed. We consider two different computation offloading models, namely the *partial* and *binary* offloading, respectively. For partial offloading, the tasks at the user are divided into three parts that are executed at the user, helper, and AP, respectively; while for binary offloading, the tasks are executed as a whole only at one of three nodes. Under this setup, we focus on a particular finite time block and develop an efficient four-slot transmission protocol to enable the *joint computation and communication cooperation*. Besides the local task computing over the whole block, the user can offload some computation tasks to the helper in the first slot, and the helper cooperatively computes these tasks in the remaining time; while in the second and third slots, the helper works as a cooperative relay to help the user offload some other tasks to the AP for remote execution in the fourth slot. For both cases with partial and binary offloading, we jointly optimize the computation and communication resources allocation at both the user and the helper (i.e., the time and transmit power allocations for offloading, and the CPU frequencies for computing), so as to minimize their total energy consumption while satisfying the user’s computation latency constraint. Although the two problems are non-convex in general, we propose efficient algorithms to solve them optimally. Numerical results show that the proposed joint computation and communication cooperation approach significantly improves the computation capacity and energy efficiency at the user and helper nodes, as compared to other benchmark schemes without such a joint design.

**Index Terms**—Mobile edge computing (MEC), joint computation and communication cooperation, resource allocation, computation offloading.

## I. INTRODUCTION

Recent advancements in the fifth-generation (5G) cellular technologies have enabled abundant applications such as the augmented reality (AR), autonomous driving, and Internet of

Part of this paper has been presented at the International Symposium on Modeling and Optimization in Mobile, Ad Hoc, and Wireless Networks, Workshop on Edge and Fog Computing for Intelligent IoT Applications, Shanghai, China, May 7–11, 2018 [1].

X. Cao, F. Wang, and J. Xu are with the School of Information Engineering, Guangdong University of Technology, Guangzhou 510006, China (e-mail: caoxwen@outlook.com, fengwang13@gdut.edu.cn, jiexu@gdut.edu.cn). F. Wang is the corresponding author.

R. Zhang is with the Department of Electrical and Computer Engineering, National University of Singapore, Singapore (e-mail: elezhang@nus.edu.sg).

S. Cui is with the Department of Electrical and Computer Engineering, University of California, Davis, USA (e-mail: sg cui@ucdavis.edu).

things (IoT). These applications usually demand ultra-low-latency communication, computation, and control among a large number of wireless devices including sensors, actuators, etc. [2]. For example, in AR applications, wireless devices need to collect image and audio information, and then implement sophisticated artificial intelligence (AI) algorithms for real-time image and speech recognition. In practice, the real-time computation tasks can be quite intensive, but wireless devices are generally of small size and only have limited communication, computation, and storage resources. Therefore, how to enhance their computation capabilities and reduce the computation latency is one crucial but challenging issue to be tackled for making these 5G applications a reality.

Mobile cloud computing (MCC) has been widely adopted as a conventional technique to enhance wireless devices’ computation capabilities, by moving the computing and data storage from these devices to the remote centralized cloud [3]. However, as the cloud servers are normally distant from wireless devices, MCC may not be able to meet the stringent computation latency requirements for emerging 5G applications. To overcome such limitations, recently mobile edge computing (MEC) has been proposed as a promising solution to provide cloud-like computing at the edge of wireless networks (e.g., access points (APs) and cellular base stations (BSs)), by deploying distributed MEC servers therein [4]–[7]. In MEC, wireless devices can offload computation-intensive and latency-critical tasks to MEC servers at APs/BSs for remote execution. As the distributed MEC servers at APs and BSs are in close proximity to these devices, the MEC is expected to achieve much lower computation latency than the MCC with centralized cloud servers.

Depending on whether the computation tasks are partitionable or not, two different types of computation offloading models, namely *binary* and *partial* offloading, have been widely adopted in the literature for MEC design [6]. In binary offloading, the computation tasks are not partitionable, and thus should be executed as a whole via either local computing by the device itself or offloading to the MEC server. In partial offloading, the computation tasks can be partitioned into two or more independent parts, which can be executed in parallel by local computing and offloading, respectively. Based on the binary and partial offloading models, there have been a handful of prior works (see, e.g., [7]–[15] and the references therein) investigating the joint computation and communication optimization to improve the performance of MEC. For example, [8] and [9] considered a single-user MEC system with dynamic task arrivals and channel fading,

in which the user jointly optimizes the local computing or offloading decisions to minimize the computation latency, subject to the computation and communication resource constraints. [10]–[12] investigated the energy-efficient design in multiuser MEC systems, in which multiple users aim to minimize their sum energy consumption subject to computation latency constraints, by jointly optimizing their computation and communication resources allocation for local computing and offloading, respectively. Furthermore, [13]–[15] proposed wireless powered MEC systems by integrating the emerging wireless power transfer (WPT) technology into MEC for self-sustainable computing, where the AP employs WPT to power the users' local computing and offloading.

Despite the recent research progress, the implementation of multiuser MEC systems still faces several technical challenges. First, in such systems, the computation resources at the MEC server and the communication resources (e.g., time, frequency, and power) at the AP might be shared or competed among multiple actively-computing users. When the number of users becomes large, the computation and communication resources allocated to each user are fundamentally limited, thus compromising the benefit of MEC. Next, due to the severe signal propagation loss over distances, far-apart users may spend much more time/frequency/power resources than nearby users for offloading; this results in a near-far user fairness issue. In order to relieve the resource limitation at APs/MEC servers and overcome the notorious near-far fairness issue in computation offloading, we propose in this paper a novel *joint computation and communication cooperation* approach in MEC systems to enable user cooperation in both computation and communication. This approach is motivated by the fact that emerging 5G wireless networks will consist of massive wireless devices each with certain local computation and communication resources; due to the bursty nature of wireless traffics, each active device is highly likely to be surrounded by a number of idle devices. In the joint computation and communication cooperation approach, nearby idle users can share their computation and communication resources to help active users improve the computation experience.

For the purpose of exposition, in this paper we consider a basic three-node MEC system, which comprises a user node, a helper node, and an AP node attached with an MEC server. We focus on the user's latency-constrained computation over a time block of finite-length. It is assumed that the user's computation tasks are required to be successfully executed before the end of this block. The joint computation and communication cooperation is implemented as follows by dividing the block into four time slots. In the first slot, the user offloads some computation tasks to the helper, which cooperatively computes them in the remaining time with computation cooperation; in the second and third slots, the helper acts as a decode-and-forward (DF) relay for cooperative communication, in order to help the user offload some other computation tasks to the AP for remote execution in the fourth slot. Under this setup, we pursue an energy-efficient MEC design via joint computation and communication resource allocations, by considering both the partial and binary offloading cases. The main results of this paper are summarized as follows.

- First, for the partial offloading case, the user's computation tasks are partitioned into three parts for local computation, offloading to helper (for cooperative computing at the helper), and offloading to AP (via the relaying of the helper for remote computing at the MEC server), respectively. In this case, we minimize the total energy consumption at both the user and the helper subject to the user's computation latency constraint, by jointly optimizing the task partition among the three nodes, the CPU frequencies for local computing at both the user and the helper, as well as the time and transmit power allocations for offloading. Although the problem under consideration is non-convex in general, we show that it can be reformulated into a convex form. Leveraging the Lagrange duality method, we obtain the globally optimal solution in a semi-closed form.
- Next, for the binary offloading case, the user should execute the non-partitionable computation tasks by choosing one among three computation modes, including local computing at the user, computation cooperation (offloading to the helper), and communication cooperation (offloading to the AP). In this case, we consider the latency-constrained energy minimization problem by choosing the computation mode, and optimize the corresponding joint computation and communication resources allocation. We present the optimal solution to this problem by first obtaining the optimal resource allocation under each given computation mode, and then determining the optimal mode with the minimum energy consumption.
- Finally, numerical results show that the proposed joint computation and communication cooperation approach significantly outperforms other benchmark schemes without such a joint design, in terms of both the computation capacity and the system energy efficiency.

It is worth noting that there have been prior studies on communication cooperation (see, e.g., [16]–[21]) or computation cooperation [22]–[25], respectively. On one hand, the cooperative communication via relaying has been extensively investigated in wireless communication systems, in which relay nodes are employed to forward the information from source to destination nodes [18], [19]. By exploiting the cooperative diversity, the relaying technique can significantly increase the communication rate and improve the communication reliability. As such, this technique has been applied in various other setups such as the wireless powered communication [20] and the wireless powered MEC systems [21]. On the other hand, cooperative computation has emerged as a viable technique in MEC systems, which enables end users to exploit computation resources at nearby wireless devices (instead of APs or BSs). For example, in the so-called device-to-device (D2D) fogging [24] and peer-to-peer (P2P) cooperative computing [25], actively-computing users can offload their computation tasks to other idle users via D2D or P2P communications for task execution. Similar computation task sharing among wireless devices has also been investigated in mobile social networks with crowdsensing [22] and in mobile wireless sensor networks [23]. However, different from these existing

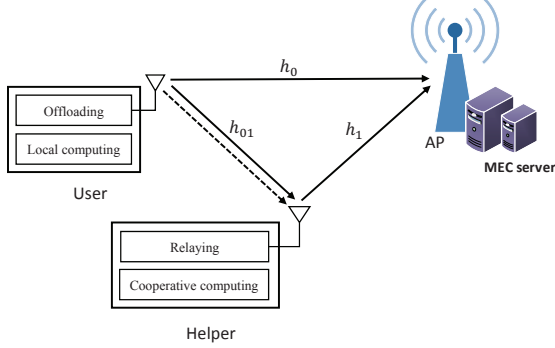


Fig. 1. A basic three-node MEC system with joint computation and communication cooperation. The dashed and solid lines indicate the tasks offloaded to the helper (for computation cooperation) and to the AP (via the helper's communication cooperation as a relay), respectively.

works with communication or computation cooperation, this work is the first attempt to pursue a *joint computation and communication cooperation* approach, by unifying both the cooperative computing and cooperative communication, for further improving the MEC performance.

The remainder of this paper is organized as follows. Section II introduces the system model. Section III formulates the latency-constrained energy minimization problems under the partial and binary offloading models, respectively. Sections IV and V present the optimal solutions to the two problems of our interests, respectively. Section VI provides numerical results, followed by the conclusion in Section VII.

## II. SYSTEM MODEL

As shown in Fig. 1, we consider a basic three-node MEC system consisting of one user node, one helper node, and one AP node with an MEC server integrated,<sup>1</sup> in which the three nodes are each equipped with one single antenna. We focus on a time block with finite duration  $T > 0$ , where the user needs to successfully execute computation tasks with  $L > 0$  task-input bits before the end of this block. We assume that the user and helper nodes are at fixed locations, and thus the wireless channels remain unchanged over this block. It is further assumed that the user node perfectly knows the channel state information (CSI) between any two nodes, the maximum transmit power of the helper node, and the computation-related information (i.e., the number of CPU cycles for computing one task-input bit, the maximum CPU frequency and/or the computing capacitance coefficient) of the helper node and the AP; accordingly, it can design and implement the proposed joint computation and communication cooperation protocol.

Specifically, without loss of generality, the  $L$  task-input bits can be divided into three parts intended for local computing, offloading to helper, and offloading to AP, respectively. Let  $l_u \geq 0$ ,  $l_h \geq 0$ , and  $l_a \geq 0$  denote the numbers of task-input

<sup>1</sup>Note that the joint computation and communication cooperation in this paper can be extended into the scenario with multiple users and multiple helpers, by efficiently pairing one helper with each user for cooperation.

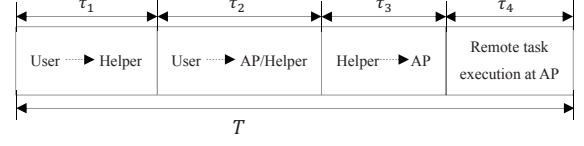


Fig. 2. MEC protocol with joint computation and communication cooperation.

bits for local computing at the user, offloading to the helper, and offloading to the AP, respectively. We then have

$$l_u + l_h + l_a = L. \quad (1)$$

We focus on two cases with partial offloading and binary offloading, respectively. In partial offloading, the computation task can be arbitrarily partitioned into subtasks. By assuming the number of subtasks are sufficiently large in this case, it is reasonable to approximate  $l_u$ ,  $l_h$ , and  $l_a$  as real numbers between 0 and  $L$  subject to (1). In binary offloading,  $l_u$ ,  $l_h$ , and  $l_a$  can only be set as 0 or  $L$ , and there is only one variable among them equal to  $L$  due to (1).

### A. MEC Protocol With Joint Computation and Communication Cooperation

As shown in Fig. 2, the duration- $T$  block is generally divided into four slots for joint computation and communication cooperation. In the first slot with duration  $\tau_1 \geq 0$ , the user offloads the  $l_h$  task-input bits to the helper, and the helper can then execute them in the remaining time with duration  $T - \tau_1$ . In the second and third slots, the helper acts as a DF relay to help the user offload  $l_a$  task-input bits to the AP. More specifically, in the second slot with duration  $\tau_2 \geq 0$ , the user broadcasts the  $l_a$  task-input bits to both the AP and the helper simultaneously; after successfully decoding the received bits, the helper forwards them to the AP in the third slot with duration  $\tau_3 \geq 0$ . After decoding the information from the user and the helper, the MEC server can remotely execute the offloaded tasks in the fourth time slot with duration  $\tau_4 \geq 0$ . As the computation results are normally of much smaller size than the input bits, the time for downloading the results to the user is negligible compared to the offloading time; hence, we ignore the downloading time in this paper. In order to ensure the computation tasks to be successfully executed before the end of this block, we have the following time constraint:

$$\tau_1 + \tau_2 + \tau_3 + \tau_4 \leq T. \quad (2)$$

In the following, we discuss the computation offloading from the user to the helper and the AP, and the computing at the three nodes, respectively.

### B. Computation Offloading

1) *Computation Offloading to Helper*: In the first slot, the user offloads  $l_h$  task-input bits to the helper with transmit power  $P_1 \geq 0$ . Let  $h_{01} > 0$  denote the channel power gain

from the user to the helper, and  $B$  the system bandwidth. Accordingly, the achievable data rate (in bits/sec) for offloading from the user to the helper is given by

$$r_{01}(P_1) = B \log_2 \left( 1 + \frac{P_1 h_{01}}{\Gamma \sigma_1^2} \right), \quad (3)$$

where  $\sigma_1^2$  represents the power of additive white Gaussian noise (AWGN) at the helper, and  $\Gamma \geq 1$  is a constant term accounting for the gap from the channel capacity due to a practical modulation and coding scheme (MCS). For simplicity,  $\Gamma = 1$  is assumed throughout this paper. Consequently, we have the number of task-input bits  $l_h$  as

$$l_h = \tau_1 r_{01}(P_1). \quad (4)$$

Furthermore, let  $P_{u,\max}$  denote the maximum transmit power at the user, and thus we have  $0 \leq P_1 \leq P_{u,\max}$ . For computation offloading, we consider the user's transmission energy as the dominant energy consumption and ignore the energy consumed by circuits in its radio-frequency (RF) chains, baseband signal processing, etc. Therefore, in the first slot, the energy consumption for the user to offload  $l_h$  task-input bits to the helper is given by

$$E_1^{\text{offl}} = \tau_1 P_1. \quad (5)$$

2) *Computation Offloading to AP Assisted by Helper*: In the second and third slots, the helper acts as a DF relay to help the user offload  $l_a$  task-input bits to the AP. Denote by  $0 \leq P_2 \leq P_{u,\max}$  the user's transmit power in the second slot. In this case, the achievable data rate from the user to the helper is given by  $r_{01}(P_2)$  with  $r_{01}(\cdot)$  defined in (3). Denoting  $h_0 > 0$  as the channel power gain from the user to the AP, the achievable data rate from the user to the AP is

$$r_0(P_2) = B \log_2 \left( 1 + \frac{P_2 h_0}{\sigma_0^2} \right), \quad (6)$$

where  $\sigma_0^2$  is the noise power at the AP receiver.

After successfully decoding the received message, the helper forwards it to the AP in the third slot with the transmit power  $0 \leq P_3 \leq P_{h,\max}$ , where  $P_{h,\max}$  denotes the maximum transmit power at the helper. Let  $h_1 > 0$  denote the channel power gain from the helper to the AP. The achievable data rate from the helper to the AP is thus

$$r_1(P_3) = B \log_2 \left( 1 + \frac{P_3 h_1}{\sigma_0^2} \right). \quad (7)$$

By combining the second and third slots, the number of  $l_a$  task-input bits offloaded to the AP via a DF relay (the helper) should satisfy [19]

$$l_a = \min (\tau_2 r_0(P_2) + \tau_3 r_1(P_3), \tau_2 r_{01}(P_2)). \quad (8)$$

As in (5), we consider the user's and helper's transmission energy consumption for offloading as the dominant energy budget in both the second and third slots. Therefore, we have

$$E_2^{\text{offl}} = \tau_2 P_2, \quad (9)$$

$$E_3^{\text{offl}} = \tau_3 P_3. \quad (10)$$

### C. Computing at User, Helper, and AP

1) *Local Computing at User*: The user executes the computation tasks with  $l_u$  task-input bits throughout the whole block with duration  $T$ . In practice, the number of CPU cycles for executing a computation task is highly dependent on various factors such as the specific applications, the number of task-input bits, as well as the hardware (e.g., CPU and memory) architectures at the computing device [26]. To characterize the most essential computation and communication tradeoff and as commonly adopted in the literature (e.g., [8], [14]), we consider that the number of CPU cycles for this task is a linear function with respect to the number of task-input bits, where  $c_u$  denotes the number of CPU cycles for computing each one task-input bit at the user. Also, let  $f_{u,n}$  denote the CPU frequency for the  $n$ -th cycle, where  $n \in \{1, \dots, c_u l_u\}$ . In practice, the CPU frequency  $f_{u,n}$  is constrained by a maximum value, denoted by  $f_{u,\max}$ , i.e.,

$$f_{u,n} \leq f_{u,\max}, \quad \forall n \in \{1, \dots, c_u l_u\}. \quad (11)$$

As the local computing for the  $l_u$  task-input bits should be accomplished before the end of the time block, we have the following computation latency requirement:

$$\sum_{n=1}^{c_u l_u} \frac{1}{f_{u,n}} \leq T. \quad (12)$$

Accordingly, the user's energy consumption for local computing is [6]

$$E_u^{\text{comp}} = \sum_{n=1}^{c_u l_u} \kappa_u f_{u,n}^2, \quad (13)$$

where  $\kappa_u$  denotes the effective capacitance coefficient that depends on the chip architecture at the user [26]. It has been shown in [13, Lemma 1] that to save the computation energy consumption with a computation latency requirement, it is optimal to set the CPU frequencies to be identical for different CPU cycles. By using this fact and letting the constraint in (12) be met with strict equality (for minimizing the computation energy consumption), we have

$$f_{u,1} = f_{u,2} = \dots = f_{u,c_u l_u} = c_u l_u / T. \quad (14)$$

Substituting (14) into (13), the user's corresponding energy consumption for local computing is re-expressed as

$$E_u^{\text{comp}} = \frac{\kappa_u c_u^3 l_u^3}{T^2}. \quad (15)$$

Combining (14) with the maximum CPU frequency constraint in (11), it follows that

$$c_u l_u \leq T f_{u,\max}. \quad (16)$$

2) *Cooperative Computing at Helper*: After receiving the offloaded  $l_h$  task-input bits in the first time slot, the helper executes the tasks during the remaining time with duration  $(T - \tau_1)$ . Let  $f_{h,n}$  and  $f_{h,\max}$  denote the CPU frequency for the  $n$ -th CPU cycle and the maximum CPU frequency at the helper, respectively. Similarly as for the local computing at the user, it is optimal for helper to set the CPU frequency for the  $n$ -th CPU cycle as  $f_{h,n} = c_h l_h / (T - \tau_1)$ ,  $n \in \{1, \dots, c_h l_h\}$ ,

where  $c_h$  is the number of CPU cycles for computing one task-input bit at the helper. Accordingly, the energy consumption for cooperative computation at the helper is given by

$$E_h^{\text{comp}} = \frac{\kappa_h c_h^3 l_h^3}{(T - \tau_1)^2}, \quad (17)$$

where  $\kappa_h$  is the effective capacitance coefficient of the helper.

Similarly as in (16), we have the constraint on the number of task-input bits as

$$c_h l_h \leq (T - \tau_1) f_{h,\text{max}}, \quad (18)$$

where  $f_{h,\text{max}}$  denotes the maximum CPU frequency for the helper.

3) *Remote Computing at AP (MEC Server)*: In the fourth slot with duration  $\tau_4$ , the MEC server at the AP executes the offloaded  $l_a$  task-input bits. In order to minimize the remote execution, we consider that the MEC server computes the offloaded tasks at its maximal CPU frequency, denoted by  $f_{a,\text{max}}$ . Hence, the time duration  $\tau_4$  for the MEC server to execute the  $l_a$  offloaded bits is

$$\tau_4 = c_a l_a / f_{a,\text{max}}, \quad (19)$$

where  $c_a$  represents the cycles required for computing one task-input bit at the AP. By substituting (19) into (2), the time allocation constraint is re-expressed as

$$\tau_1 + \tau_2 + \tau_3 + c_a l_a / f_{a,\text{max}} \leq T. \quad (20)$$

### III. PROBLEM FORMULATION

In this paper, we pursue an energy-efficient design for the three-node MEC system. As the AP normally has reliable power supply, we focus on the energy consumption at the wireless devices side (including the user and the helper) as the performance metric. In particular, we aim to minimize the total energy consumption at both the user and the helper (i.e.,  $\sum_{i=1}^3 E_i^{\text{offl}} + E_u^{\text{comp}} + E_h^{\text{comp}}$ ), subject to the user's computation latency constraint, by optimizing the task partition and their joint computation and communication resources allocation. The design variables include the allocation of the time slots  $\tau \triangleq [\tau_1, \tau_2, \tau_3]$ , the task partition  $\mathbf{l} \triangleq [l_u, l_h, l_a]$ , and the offloading power allocation  $\mathbf{P} \triangleq [P_1, P_2, P_3]$ .

In the case with partial offloading, the latency-constrained energy minimization problem is formulated as

$$(P1) : \min_{\mathbf{P}, \tau, \mathbf{l}} \frac{\kappa_u c_u^3 l_u^3}{T^2} + \frac{\kappa_h c_h^3 l_h^3}{(T - \tau_1)^2} + \sum_{i=1}^3 \tau_i P_i \quad (21a)$$

$$\text{s.t. } l_h \leq \tau_1 r_{01}(P_1) \quad (21b)$$

$$l_a \leq \min(\tau_2 r_0(P_2) + \tau_3 r_1(P_3), \tau_2 r_{01}(P_2)) \quad (21c)$$

$$0 \leq P_j \leq P_{u,\text{max}}, \forall j \in \{1, 2\} \quad (21d)$$

$$0 \leq P_3 \leq P_{h,\text{max}} \quad (21e)$$

$$0 \leq \tau_i \leq T, \forall i \in \{1, 2, 3\} \quad (21f)$$

$$l_u \geq 0, l_h \geq 0, l_a \geq 0 \quad (21g)$$

(1), (16), (18), and (20),

where (1) denotes the task partition constraint, (16) and (18) are the maximum CPU frequency constraints at the user and

the helper, respectively, (20) denotes the time allocation constraint, (21b) and (21c) denote the constraints for the numbers of the offloaded bits from the user to the helper and to the AP, respectively. Note that in (P1), we replace the two equalities in (4) and (8) as two inequality constraints (21b) and (21c). It is clear that constraints (21b) and (21c) should be met with strict equality at optimality of (P1). Also note that problem (P1) is non-convex and difficult to be optimally solved, due to the coupling of  $\tau_i$  and  $P_i$  in the objective function (21a) and the constraints (21b) and (21c). Nonetheless, in Section IV we will transform (P1) into an equivalent convex problem and then present an efficiently algorithm to obtain the optimal solution of problem (P1).

In the case with binary offloading, the latency-constrained energy minimization problem is formulated as

$$(P2) : \min_{\mathbf{P}, \tau, \mathbf{l}} \frac{\kappa_u c_u^3 l_u^3}{T^2} + \frac{\kappa_h c_h^3 l_h^3}{(T - \tau_1)^2} + \sum_{i=1}^3 \tau_i P_i \quad (22a)$$

$$\text{s.t. } l_u \in \{0, L\}, l_h \in \{0, L\}, l_a \in \{0, L\} \quad (22b)$$

(1), (16), (18), (20), and (21b-f).

Note that problem (P2) is a mixed-integer nonlinear program (MINLP) [27] due to the involvement of integer variables  $l_u$ ,  $l_h$ , and  $l_a$ . In Section V, we will develop an efficient algorithm to solve (P2) optimally by examining three computation modes, respectively.

#### A. Feasibility of (P1) and (P2)

Before solving problems (P1) and (P2), we first check their feasibility to examine whether the three-node MEC system can support the latency-constrained task execution or not. Let  $L_{\text{max}}^{(1)}$  and  $L_{\text{max}}^{(2)}$  denote the maximum numbers of task-input bits supported by the MEC system within the duration- $T$  block under the partial and binary offloading cases, respectively. It is evident that if  $L_{\text{max}}^{(1)} \geq L$  (or  $L_{\text{max}}^{(2)} \geq L$ ), then problem (P1) (or (P2)) is feasible; otherwise, the corresponding problem is not feasible. Therefore, the feasibility checking of (P1) and (P2) corresponds to determining  $L_{\text{max}}^{(1)}$  and  $L_{\text{max}}^{(2)}$ , respectively.

First, consider the partial offloading case. The maximum number of task-input bits  $L_{\text{max}}^{(1)}$  is attained when all the three nodes fully use their available communication and computation resources, i.e., by setting  $P_1 = P_2 = P_{u,\text{max}}$ ,  $P_3 = P_{h,\text{max}}$ , and letting the constraints (16), (18), (20), and (21c) be met with the strict equality in problem (P1). As a result,  $L_{\text{max}}^{(1)}$  is the optimal value of the following problem:

$$L_{\text{max}}^{(1)} \triangleq \max_{\tau, \mathbf{l}} l_u + l_h + l_a \quad (23)$$

$$\text{s.t. } \tau_1 + \tau_2 + \tau_3 + c_a l_a / f_{a,\text{max}} = T$$

$$l_h \leq \tau_1 r_{01}(P_{u,\text{max}}), l_a \leq \tau_2 r_{01}(P_{u,\text{max}})$$

$$c_u l_u / T = f_{u,\text{max}}, c_h l_h / (T - \tau_1) = f_{h,\text{max}}$$

$$\tau_2 r_0(P_{u,\text{max}}) + \tau_3 r_1(P_{h,\text{max}}) = \tau_2 r_{01}(P_{u,\text{max}})$$

$$(21f) \text{ and } (21g).$$

Note that problem (23) is a linear program (LP) and can thus be efficiently solved via standard convex optimization techniques such as the interior point method [29]. By comparing  $L_{\text{max}}^{(1)}$  versus  $L$ , the feasibility of (P1) is checked.

Next, consider the binary offloading case. The user's computation tasks can only be executed by one of the three computation modes, namely the *local computing*, *computation cooperation* (offloading to helper), and *communication cooperation* (offloading to AP). For the three modes, the maximum numbers of supportable task-input bits can be obtained as follows.

- For the local-computing mode, we have  $l_h = l_a = 0$ . With the maximum CPU frequency  $f_{u,\max}$  and setting (16) to be tight, the maximum supportable number of task-input bits is thus

$$l_{u,\max}^{(2)} = \frac{T f_{u,\max}}{c_u}. \quad (24)$$

- For the computation-cooperation mode, we have  $l_u = l_a = 0$ . By setting the user's transmit power as  $P_1 = P_{u,\max}$ , and making the constraints (18) and (21b) be tight in (P2), the maximum number of task-input bits is thus

$$l_{h,\max}^{(2)} = \tau_1^b r_{01}(P_{u,\max}), \quad (25)$$

where  $\tau_1^b = T f_{h,\max} / (c_h r_{01}(P_{u,\max}) + f_{h,\max})$  corresponds to the optimal time allocation for offloading.

- For the communication-cooperation mode, we have  $l_u = l_h = 0$ ,  $P_2 = P_{u,\max}$ , and  $P_3 = P_{h,\max}$  in (P2). The maximum number of task-input bits  $l_{a,\max}^{(2)}$  is obtained by solving the following LP:

$$\begin{aligned} l_{a,\max}^{(2)} &\triangleq \arg \max_{\tau_2, \tau_3, l_a} l_a & (26) \\ \text{s.t. } l_a &\leq \min \left( \tau_2 r_{01}(P_{u,\max}), \right. \\ &\quad \left. \tau_2 r_0(P_{u,\max}) + \tau_3 r_1(P_{h,\max}) \right) \\ &\quad \tau_2 + \tau_3 + c_a l_a / f_{a,\max} \leq T \\ &\quad 0 \leq \tau_2 \leq T, \quad 0 \leq \tau_3 \leq T. \end{aligned}$$

Based on (24)–(26), the maximum number of supportable task-input bits with binary offloading is given by

$$L_{\max}^{(2)} = \max \left( l_{u,\max}^{(2)}, l_{h,\max}^{(2)}, l_{a,\max}^{(2)} \right). \quad (27)$$

By comparing  $L_{\max}^{(2)}$  with  $L$ , the feasibility of (P2) is checked.

By comparing  $L_{\max}^{(1)}$  and  $L_{\max}^{(2)}$ , we show that  $L_{\max}^{(1)} \geq L_{\max}^{(2)}$ . This is expected since that any feasible solution to (P2) is always feasible for (P1) but the reverse is generally not true. The partial offloading case can better utilize the distributed computation resources at different nodes, and thus achieves higher computation capacity than the binary offloading case.

#### IV. OPTIMAL SOLUTION TO (P1)

This section focuses on solving problem (P1) in the partial offloading case.

To this end, we introduce a set of auxiliary variables  $\mathbf{E} \triangleq [E_1, E_2, E_3]$  with  $E_i = P_i \tau_i$ ,  $i \in \{1, 2, 3\}$ . Then it holds that  $P_i = E_i / \tau_i$  if  $\tau_i > 0$ , and  $P_i = 0$  if either  $E_i = 0$  or  $\tau_i = 0$

holds,  $i \in \{1, 2, 3\}$ . By substituting  $P_i = E_i / \tau_i$ ,  $i \in \{1, 2, 3\}$ , problem (P1) can be reformulated as

$$(P1.1) : \min_{\mathbf{E}, \boldsymbol{\tau}, \mathbf{l}} \frac{\kappa_u c_u^3 l_u^3}{T^2} + \frac{\kappa_h c_h^3 l_h^3}{(T - \tau_1)^2} + \sum_{i=1}^3 E_i \quad (28a)$$

$$\text{s.t. } l_h \leq \tau_1 r_{01} \left( \frac{E_1}{\tau_1} \right) \quad (28b)$$

$$l_a \leq \tau_2 r_0 \left( \frac{E_2}{\tau_2} \right) + \tau_3 r_1 \left( \frac{E_3}{\tau_3} \right) \quad (28c)$$

$$l_a \leq \tau_2 r_{01} \left( \frac{E_2}{\tau_2} \right) \quad (28d)$$

$$0 \leq E_j \leq \tau_j P_{u,\max}, \quad \forall j \in \{1, 2\} \quad (28e)$$

$$0 \leq E_3 \leq \tau_3 P_{h,\max} \quad (28f)$$

(1), (16), (18), (20), (21f), and (21g),

where both (28c) and (28d) follow from (21c). The function  $r_j(x)$  is a concave function with respect to  $x \geq 0$  for any  $j \in \{0, 1, 01\}$ , and thus its perspective function  $x r_j(\frac{y}{x})$  is jointly concave with respect to  $x > 0$  and  $y \geq 0$  [29]. As a result, the sets defined by constraints (28b)–(28d) become convex. The function  $l^3 / \tau^2$  is a convex function with respect to  $l \geq 0$  and  $\tau > 0$ , and hence the term  $\kappa_h c_h^3 l_h^3 / (T - \tau_1)^2$  in the objective function is jointly convex with respect to  $l_h \geq 0$  and  $0 \leq \tau_1 < T$ . Therefore, problem (P1.1) is convex and can thus be optimally solved by the interior point method [29]. Alternatively, to gain more essential engineering insights, in the following we leverage the Lagrange duality method to obtain a well-structured optimal solution for (P1.1).

Let  $\lambda_1 \geq 0$ ,  $\lambda_2 \geq 0$ , and  $\lambda_3 \geq 0$  denote the dual variables associated with the constraints in (28b–d), respectively,  $\mu_1 \geq 0$  and  $\mu_2 \in \mathbb{R}$  be the dual variables associated with the constraints in (20) and (1), respectively. Define  $\boldsymbol{\lambda} \triangleq [\lambda_1, \lambda_2, \lambda_3]$  and  $\boldsymbol{\mu} \triangleq [\mu_1, \mu_2]$ . The partial Lagrangian of problem (P1.1) is given by

$$\begin{aligned} \mathcal{L}(\mathbf{E}, \boldsymbol{\tau}, \mathbf{l}, \boldsymbol{\lambda}, \boldsymbol{\mu}) &= \sum_{i=1}^3 E_i + \mu_1 \tau_1 + \frac{\kappa_h c_h^3 l_h^3}{(T - \tau_1)^2} + (\lambda_1 - \mu_2) l_h \\ &\quad - \lambda_1 \tau_1 r_{01} \left( \frac{E_1}{\tau_1} \right) - \lambda_2 \tau_2 r_0 \left( \frac{E_2}{\tau_2} \right) - \lambda_3 \tau_2 r_{01} \left( \frac{E_2}{\tau_2} \right) \\ &\quad + \mu_1 \tau_2 - \lambda_2 \tau_3 r_1 \left( \frac{E_3}{\tau_3} \right) + \mu_1 \tau_3 + \frac{\kappa_u c_u^3 l_u^3}{T^2} - \mu_2 l_u \\ &\quad + (\lambda_2 + \lambda_3 + \mu_1 c_a / f_{a,\max} - \mu_2) l_a - \mu_1 T + \mu_2 L. \end{aligned}$$

Then the dual function of problem (P1.1) is given by

$$\begin{aligned} g(\boldsymbol{\lambda}, \boldsymbol{\mu}) &= \min_{\mathbf{E}, \boldsymbol{\tau}, \mathbf{l}} \mathcal{L}(\mathbf{E}, \boldsymbol{\tau}, \mathbf{l}, \boldsymbol{\lambda}, \boldsymbol{\mu}) & (29) \\ \text{s.t. } (16), (18), (21f), (21g), (28e), \text{ and } (28f). \end{aligned}$$

**Lemma 4.1:** In order for  $g(\boldsymbol{\lambda}, \boldsymbol{\mu})$  to be bounded from below, it must hold that  $\lambda_1 - \mu_2 \geq 0$  and  $\lambda_2 + \lambda_3 + \mu_1 c_a / f_{a,\max} - \mu_2 \geq 0$ .

*Proof:* See Appendix A. ■

Consequently, the dual problem of (P1.1) is given by

$$\begin{aligned} (D1.1) : \max_{\boldsymbol{\lambda}, \boldsymbol{\mu}} \quad & g(\boldsymbol{\lambda}, \boldsymbol{\mu}) & (30) \\ \text{s.t. } \mu_1 \geq 0, \quad & \lambda_i \geq 0, \quad \forall i \in \{1, 2, 3\} \end{aligned}$$

$$\begin{aligned}\lambda_1 - \mu_2 &\geq 0 \\ \lambda_2 + \lambda_3 + \mu_1 c_a / f_{a,\max} - \mu_2 &\geq 0.\end{aligned}$$

For notational convenience, denote  $\mathcal{X}$  as the set of  $(\lambda, \mu)$  characterized by the constraints in (30).

Since problem (P1.1) is convex and satisfies the Slater's condition, strong duality holds between problems (P1.1) and (D1.1) [29]. As a result, one can solve (P1.1) by equivalently solving its dual problem (D1.1). In the following, we first evaluate the dual function  $g(\lambda, \mu)$  under any given  $(\lambda, \mu) \in \mathcal{X}$ , and then obtain the optimal dual variables to maximize  $g(\lambda, \mu)$ . Denote  $(E^*, \tau^*, l^*)$  as the optimal solution to problem (29) under any given  $(\lambda, \mu) \in \mathcal{X}$ ,  $(E^{\text{opt1}}, \tau^{\text{opt1}}, l^{\text{opt1}})$  as the optimal primal solution to problem (P1.1), and  $(\lambda^{\text{opt1}}, \mu^{\text{opt1}})$  as the optimal dual solution to problem (D1.1).

### A. Derivation of Dual Function $g(\lambda, \mu)$

First, we obtain  $g(\lambda, \mu)$  by solving (29) under any given  $(\lambda, \mu) \in \mathcal{X}$ . Equivalently, (29) can be decomposed into the following five subproblems.

$$\begin{aligned}\min_{E_1, \tau_1, l_h} \quad & E_1 + \mu_1 \tau_1 - \lambda_1 \tau_1 r_{01} \left( \frac{E_1}{\tau_1} \right) + \frac{\kappa_h c_h^3 l_h^3}{(T - \tau_1)^2} + (\lambda_1 - \mu_2) l_h \\ \text{s.t. (18), } & 0 \leq E_1 \leq \tau_1 P_{u,\max}, \quad 0 \leq \tau_1 \leq T, \quad l_h \geq 0.\end{aligned}\quad (31)$$

$$\begin{aligned}\min_{E_2, \tau_2} \quad & E_2 + \mu_1 \tau_2 - \lambda_2 \tau_2 r_0 \left( \frac{E_2}{\tau_2} \right) - \lambda_3 \tau_2 r_{01} \left( \frac{E_2}{\tau_2} \right) \\ \text{s.t. } & 0 \leq E_2 \leq \tau_2 P_{u,\max}, \quad 0 \leq \tau_2 \leq T.\end{aligned}\quad (32)$$

$$\begin{aligned}\min_{E_3, \tau_3} \quad & E_3 + \mu_1 \tau_3 - \lambda_2 \tau_3 r_1 \left( \frac{E_3}{\tau_3} \right) \\ \text{s.t. } & 0 \leq E_3 \leq \tau_3 P_{h,\max}, \quad 0 \leq \tau_3 \leq T.\end{aligned}\quad (33)$$

$$\begin{aligned}\min_{l_u \geq 0} \quad & \frac{\kappa_u c_u^3 l_u^3}{T^2} - \mu_2 l_u \\ \text{s.t. } & c_u l_u \leq T f_{u,\max}.\end{aligned}\quad (34)$$

$$\min_{0 \leq l_a \leq L} \quad (\lambda_2 + \lambda_3 + \mu_1 c_a / f_{a,\max} - \mu_2) l_a. \quad (35)$$

The optimal solutions to problems (31)–(35) are presented in the following Lemmas 4.2–4.6, respectively. As these lemmas can be similarly proved via the Karush-Kuhn-Tucker (KKT) conditions [29], we only show the proof of Lemma 4.2 in Appendix B and omit the proofs of Lemmas 4.3–4.6 for brevity.

Lemma 4.2: Under given  $(\lambda, \tau) \in \mathcal{X}$ , the optimal solution  $(E_1^*, \tau_1^*, l_h^*)$  to problem (31) satisfies

$$E_1^* = P_1^* \tau_1^*, \quad (36)$$

$$l_h^* = M_1^* (T - \tau_1^*), \quad (37)$$

$$\tau_1^* \begin{cases} = T, & \text{if } \rho_1 < 0 \\ \in [0, T], & \text{if } \rho_1 = 0 \\ = 0, & \text{if } \rho_1 > 0, \end{cases} \quad (38)$$

where  $P_1^* = \left[ \frac{\lambda_1 B}{\ln 2} - \frac{\sigma_1^2}{h_{01}} \right]_0^{P_{u,\max}}$  with  $[x]_b^a \triangleq \min\{a, \max\{x, b\}\}$ , and

$$M_1^* \triangleq \begin{cases} \left[ \sqrt{\frac{\mu_2 - \lambda_1}{3\kappa_h c_h^3}} \right]_0^{\frac{f_{h,\max}}{c_h}}, & \text{if } \mu_2 - \lambda_1 \geq 0 \\ 0, & \text{if } \mu_2 - \lambda_1 < 0, \end{cases} \quad (39)$$

$$\begin{aligned}\rho_1 = & \mu_1 - \lambda_1 r_{01}(P_1^*) + 2\kappa_h (c_h M_1^*)^3 + \frac{\lambda_1 B P_1^* h_{01} / \sigma_1^2}{(1 + P_1^* h_{01} / \sigma_1^2) \ln 2} \\ & - \alpha_1 P_{u,\max} + \frac{\beta_1 f_{h,\max}}{c_h},\end{aligned}\quad (40)$$

$$\alpha_1 \triangleq \begin{cases} 0, & \text{if } P_1^* < P_{u,\max} \\ \frac{\lambda_1 B h_{01} / \sigma_1^2}{\ln 2 (1 + P_1^* h_{01} / \sigma_1^2)} - 1, & \text{if } P_1^* = P_{u,\max}, \end{cases} \quad (41)$$

$$\beta_1 \triangleq \begin{cases} 0, & \text{if } M_1^* < \frac{f_{h,\max}}{c_h} \\ \mu_2 - \lambda_1 - 3\kappa_h c_h^3 (M_1^*)^2, & \text{if } M_1^* = \frac{f_{h,\max}}{c_h}. \end{cases} \quad (42)$$

*Proof:* See Appendix B.  $\blacksquare$

Lemma 4.3: Under given  $(\lambda, \tau) \in \mathcal{X}$ , the optimal solution  $(E_2^*, \tau_2^*)$  to problem (32) satisfies

$$E_2^* = P_2^* \tau_2^*, \quad (43)$$

$$\tau_2^* \begin{cases} = T, & \text{if } \rho_2 < 0 \\ \in [0, T], & \text{if } \rho_2 = 0 \\ = 0, & \text{if } \rho_2 > 0,\end{cases} \quad (44)$$

where  $P_2^* = \left[ \frac{\sqrt{v^2 - 4uw} - v}{2u} \right]_0^{P_{u,\max}}$  with  $u = \frac{\ln 2}{B} \frac{h_0}{\sigma_0^2} \frac{h_{01}}{\sigma_1^2}$ ,  $v = \frac{\ln 2}{B} \left( \frac{h_0}{\sigma_0^2} + \frac{h_{01}}{\sigma_1^2} \right) - (\lambda_2 + \lambda_3) \frac{h_0}{\sigma_0^2} \frac{h_{01}}{\sigma_1^2}$ ,  $w = \frac{\ln 2}{B} - \lambda_2 \frac{h_0}{\sigma_0^2} - \lambda_3 \frac{h_{01}}{\sigma_1^2}$ ,  $\rho_2 = \frac{\lambda_2 B P_2^* \frac{h_0}{\sigma_0^2}}{(1 + P_2^* \frac{h_0}{\sigma_0^2}) \ln 2} - \lambda_3 r_{01}(P_2^*) + \frac{\lambda_3 B P_2^* \frac{h_{01}}{\sigma_1^2}}{(1 + P_2^* \frac{h_{01}}{\sigma_1^2}) \ln 2} - \alpha_2 P_{u,\max}$ , and

$$\alpha_2 = \begin{cases} 0, & \text{if } P_2^* < P_{u,\max} \\ \frac{\lambda_3 B \frac{h_{01}}{\sigma_1^2}}{(1 + P_2^* \frac{h_{01}}{\sigma_1^2}) \ln 2} + \frac{\lambda_2 B \frac{h_0}{\sigma_0^2}}{(1 + P_2^* \frac{h_0}{\sigma_0^2}) \ln 2} - 1, & \text{if } P_2^* = P_{u,\max}.\end{cases}$$

Lemma 4.4: Under given  $(\lambda, \tau) \in \mathcal{X}$ , the optimal solution  $(E_3^*, \tau_3^*)$  to problem (33) satisfies

$$E_3^* = P_3^* \tau_3^*, \quad (45)$$

$$\tau_3^* \begin{cases} = T, & \text{if } \rho_3 < 0 \\ \in [0, T], & \text{if } \rho_3 = 0 \\ = 0, & \text{if } \rho_3 > 0,\end{cases} \quad (46)$$

where  $P_3^* = \left[ \frac{\lambda_2 B}{\ln 2} - \frac{\sigma_1^2}{h_1} \right]_0^{P_{h,\max}}$  and  $\rho_3 = \mu_1 + \frac{\lambda_2 B P_3^* \frac{h_1}{\sigma_1^2}}{(1 + P_3^* \frac{h_1}{\sigma_1^2}) \ln 2} - \lambda_2 r_1(P_3^*) - \alpha_3 P_{h,\max}$  with

$$\alpha_3 = \begin{cases} 0, & \text{if } P_3^* < P_{h,\max} \\ \frac{\lambda_2 B h_1 / \sigma_0^2}{(1 + P_3^* h_1 / \sigma_0^2) \ln 2} - 1, & \text{if } P_3^* = P_{h,\max}.\end{cases}$$

Lemma 4.5: For given  $(\lambda, \tau) \in \mathcal{X}$ , the optimal solution  $l_u^*$  to problem (34) is

$$l_u^* = \left[ T \sqrt{\frac{\mu_2}{3\kappa_u c_u^3}} \right]_0^{\frac{T f_{u,\max}}{c_u}}. \quad (47)$$

Lemma 4.6: For given  $(\lambda, \tau) \in \mathcal{X}$ , the optimal solution  $l_a^*$  to problem (35) is

$$l_a^* \begin{cases} = 0, & \text{if } \lambda_2 + \lambda_3 + \mu_1 c_a / f_{a,\max} - \mu_2 > 0 \\ \in [0, L], & \text{if } \lambda_2 + \lambda_3 + \mu_1 c_a / f_{a,\max} - \mu_2 = 0 \\ = L, & \text{if } \lambda_2 + \lambda_3 + \mu_1 c_a / f_{a,\max} - \mu_2 < 0. \end{cases} \quad (48)$$

Remark 4.1: Note that in (38), (44), (46), and (48), if  $\rho_i = 0$  (for any  $i \in \{1, 2, 3\}$ ) or  $\lambda_2 + \lambda_3 + \mu_1 c_a / f_{a,\max} - \mu_2 = 0$ , then the optimal solution  $\tau_i^*$  or  $l_a^*$  is non-unique in general. In this case, we choose  $\tau_i^* = 0$  and  $l_a^* = 0$  for the purpose of evaluating the dual function  $g(\lambda, \mu)$ . Such choices may not be feasible or optimal for problem (P1.1). To tackle this issue, we use an additional step in Section IV-C later to find the primal optimal  $\tau_i^*$ 's and  $l_a^*$  for (P1.1).

By combining Lemmas 4.2–4.6, the dual function  $g(\lambda, \mu)$  is evaluated for any given  $(\lambda, \mu) \in \mathcal{X}$ .

### B. Obtaining $\lambda^{\text{opt1}}$ and $\mu^{\text{opt1}}$ to Maximize $g(\lambda, \mu)$

Next, we search over  $(\lambda, \mu) \in \mathcal{X}$  to maximize  $g(\lambda, \mu)$  for solving problem (D1.1). Since the dual function  $g(\lambda, \mu)$  is concave but non-differentiable in general, one can use subgradient based methods such as the ellipsoid method [28], to obtain the optimal  $\lambda^{\text{opt1}}$  and  $\mu^{\text{opt1}}$  for (D1.1). For the objective function in (29), the subgradient with respect to  $(\lambda, \mu)$  is

$$\begin{aligned} & \left[ l_h^* - \tau_1^* r_{01} \left( \frac{E_1^*}{\tau_1^*} \right), l_a^* - \tau_2^* r_0 \left( \frac{E_2^*}{\tau_2^*} \right) - \tau_3^* r_1 \left( \frac{E_3^*}{\tau_3^*} \right), \right. \\ & \left. l_a^* - \tau_2^* r_{01} \left( \frac{E_2^*}{\tau_2^*} \right), \sum_{i=1}^3 \tau_i^* + \frac{l_a^* c_a}{f_{a,\max}} - T, L - l_u^* - l_h^* - l_a^* \right]. \end{aligned}$$

For the constraints  $\mu_1 \geq 0$  and  $\lambda_i \geq 0$ , the subgradients are  $e_4$  and  $e_i$ ,  $i \in \{1, 2, 3\}$ , respectively, where  $e_i$  is the unit vector with one in the  $i$ -th entry and zeros elsewhere in  $\mathbb{R}^5$ .

### C. Optimal Primal Solution to (P1)

With  $\lambda^{\text{opt1}}$  and  $\mu^{\text{opt1}}$  obtained, it remains to determine the optimal solution to problem (P1.1) (and thus (P1)). By replacing  $\lambda$  and  $\mu$  in Lemmas 4.2–4.6 as  $\lambda^{\text{opt1}}$  and  $\mu^{\text{opt1}}$ , we denote the corresponding  $P_i^*$ 's,  $l_u^*$ , and  $M_1^*$  as  $P_i^{\text{opt1}}$ 's,  $l_u^{\text{opt1}}$ , and  $M_1^{\text{opt1}}$ , respectively. Accordingly,  $\mathbf{P}^{\text{opt1}} = [P_1^{\text{opt1}}, P_2^{\text{opt1}}, P_3^{\text{opt1}}]$  corresponds to the optimal solution of  $\mathbf{P}$  to problem (P1), and  $l_u^{\text{opt1}}$  corresponds to the optimal solution of  $l_u$  to both problems (P1) and (P1.1). Nevertheless, due to the nonuniqueness of  $\tau_i^*$ 's and  $l_a^*$ , we implement an additional step to construct the optimal solution of other variables to problem (P1). With  $\mathbf{P}^{\text{opt1}}$ ,  $M_1^{\text{opt1}}$ , and  $l_u^{\text{opt1}}$ , the optimal solution must satisfy  $l_h = M_1^{\text{opt1}}(T - \tau_1)$  and  $E_i = P_i^{\text{opt1}}\tau_i$ ,  $i \in \{1, 2, 3\}$ . By substituting them in (P1) or (P1.1), we have the following LP to obtain  $\tau^{\text{opt1}}$  and  $l_a^{\text{opt1}}$ :

$$\begin{aligned} & \min_{\tau, l_a \geq 0} \kappa_h (c_h M_1^{\text{opt1}})^3 (T - \tau_1) + \sum_{i=1}^3 \tau_i P_i^{\text{opt1}} \quad (49) \\ & \text{s.t.} \quad M_1^{\text{opt1}}(T - \tau_1) \leq \tau_1 r_{01}(P_1^{\text{opt1}}) \\ & \quad l_a \leq \tau_2 r_0(P_2^{\text{opt1}}) + \tau_3 r_1(P_3^{\text{opt1}}) \\ & \quad l_a \leq \tau_2 r_{01}(P_2^{\text{opt1}}) \end{aligned}$$

$$\begin{aligned} & M_1^{\text{opt1}}(T - \tau_1) + l_a + l_u^{\text{opt1}} = L \\ & 0 \leq \tau_i \leq T, \forall i \in \{1, 2, 3\}, \text{ and (20).} \end{aligned}$$

The LP in (49) can be efficiently solved by the interior-point method [29]. By combining  $\tau^{\text{opt1}}$ ,  $l_h^{\text{opt1}}$ , and  $l_u^{\text{opt1}}$ , together with  $\mathbf{P}^{\text{opt1}}$  and  $l_a^{\text{opt1}}$ , the optimal solution to problem (P1) is finally found. In summary, we present Algorithm 1 for optimally solving problem (P1) under the partial offloading case in Table I.

TABLE I  
ALGORITHM 1 FOR OPTIMALLY SOLVING PROBLEM (P1)

---

- a) Initialization: Given an ellipsoid  $\mathcal{E}((\lambda, \mu), \mathbf{A})$  containing  $(\lambda^{\text{opt1}}, \mu^{\text{opt1}})$ , where  $(\lambda, \mu)$  is the center point of  $\mathcal{E}$  and the positive definite matrix  $\mathbf{A}$  characterizes the size of  $\mathcal{E}$ .
- b) Repeat:
  - 1) Obtain  $\mathbf{P}^*$ ,  $\mathbf{E}^*$ ,  $\tau^*$ , and  $l^*$  with  $(\lambda, \mu) \in \mathcal{X}$  according to Lemmas 4.2–4.6;
  - 2) Compute the subgradients of  $g(\lambda, \mu)$ , then update  $\lambda$  and  $\mu$  using the ellipsoid method [28].
- c) Until  $\lambda$  and  $\mu$  converge with a prescribed accuracy.
- d) Set  $(\lambda^{\text{opt1}}, \mu^{\text{opt1}}) \leftarrow (\lambda, \mu)$ .
- e) Output: Obtain  $\mathbf{P}^{\text{opt1}}$  and  $l_u^{\text{opt1}}$  based on Lemmas 4.2–4.5 by replacing  $\lambda$  and  $\mu$  as  $\lambda^{\text{opt1}}$  and  $\mu^{\text{opt1}}$ , and then compute  $\tau^{\text{opt1}}$ ,  $l_h^{\text{opt1}}$ , and  $l_a^{\text{opt1}}$  by solving the LP in (49).

---

Remark 4.2: Based on the optimal solution to (P1) in semi-closed form, we have the following engineering insights on the optimal joint computation and communication cooperation.

- As for local computing, it follows from Lemma 4.5 that the number of task-input bits  $l_u^{\text{opt1}}$  for local computing generally increases as the block length  $T$  becomes large. This shows that the user prefers locally computing more tasks when the computation latency becomes loose, as will be validated in numerical results later.
- As for cooperative computation (or offloading to helper), it is evident based on Lemma 4.2 that the offloading power  $P_1^{\text{opt1}}$  in the first slot increases as the corresponding channel power gain  $h_{01}$  becomes stronger. This is intuitively expected, since the marginal energy consumption for offloading from the user to the helper reduces in this case, and thus the user prefers offloading more tasks to the helper for cooperative computation.
- As for cooperative communication (or offloading to AP), it is observed from Lemma 4.3 and 4.4 that the offloading power  $P_2^{\text{opt1}}$  in the second slot is dependent on both  $h_{01}$  and  $h_0$ , while  $P_3^{\text{opt1}}$  in the third slot increases as  $h_1$  becomes large.

## V. OPTIMAL SOLUTION TO (P2)

In this section, we focus on optimally solving problem (P2) in the binary offloading case. Due to the constraints in (1) and (22b), there exist in total three computation modes for the task execution, including the local computing (with  $l_u = L$  and  $l_h = l_a = 0$ ), the computation cooperation (with  $l_h = L$  and  $l_u = l_a = 0$ ), and the communication cooperation (with  $l_a = L$  and  $l_u = l_h = 0$ ). In the following, we optimally solve (P2) by first obtaining the energy consumption under each of the three computation modes, and then choosing the best mode with the minimum energy consumption.

1) *Local-Computing Mode*: The local-computing mode is feasible only when  $l_{u,\max}^{(2)} \geq L$ , with  $l_{u,\max}^{(2)}$  given in (24). In this case, by substituting  $l_u = L$  and  $l_h = l_a = 0$  in (P2), we have the optimal transmit power and time allocation as  $\mathbf{P} = \mathbf{0}$  and  $\boldsymbol{\tau} = \mathbf{0}$ , respectively. Therefore, the minimum energy consumption by the user in this mode is

$$E_u^{\text{opt2}} = \frac{\kappa_u c_u^3 L^3}{T^2}. \quad (50)$$

2) *Computation-Cooperation Mode*: The computation-cooperation mode is feasible only when  $l_{h,\max}^{(2)} \geq L$ , with  $l_{h,\max}^{(2)}$  given in (25). Substituting  $l_h = L$  and  $l_u = l_a = 0$  into (P2), it then follows that  $P_2 = P_3 = 0$  and  $\tau_2 = \tau_3 = 0$ . Consequently, problem (P2) is reduced as

$$\min_{P_1, \tau_1} \tau_1 P_1 + \frac{\kappa_h c_h^3 L^3}{(T - \tau_1)^2} \quad (51a)$$

$$\text{s.t. } L \leq \tau_1 r_{01}(P_1) \quad (51b)$$

$$c_h L \leq (T - \tau_1) f_{h,\max} \quad (51c)$$

$$0 \leq \tau_1 \leq T, 0 \leq P_1 \leq P_{u,\max}. \quad (51d)$$

Note that at the optimality of (51), the constraint (51b) must be tight. It thus follows that  $P_1 = \left(2^{\frac{L}{B\tau_1}} - 1\right) \frac{\sigma_1^2}{h_{01}}$ . Accordingly, problem (51) is further reduced as the following univariable convex optimization problem:

$$\begin{aligned} \tau_1^{\text{opt2}} &\triangleq \arg \min_{\tau_1} \left(2^{\frac{L}{B\tau_1}} - 1\right) \frac{\tau_1 \sigma_1^2}{h_{01}} + \frac{\kappa_h c_h^3 L^3}{(T - \tau_1)^2} \quad (52) \\ \text{s.t. } &\left(2^{\frac{L}{B\tau_1}} - 1\right) \frac{\sigma_1^2}{h_{01}} \leq P_{u,\max} \\ &0 \leq \tau_1 \leq T - \frac{c_h L}{f_{h,\max}}, \end{aligned}$$

where the optimal solution  $\tau_1^{\text{opt2}}$  can be efficiently found via a simple bisectional search [29]. With  $\tau_1^{\text{opt2}}$  obtained, the sum energy consumption at the user and the helper is given by

$$E_h^{\text{opt2}} = \left(2^{\frac{L}{B\tau_1^{\text{opt2}}}} - 1\right) \frac{\tau_1^{\text{opt2}} \sigma_1^2}{h_{01}} + \frac{\kappa_h c_h^3 L^3}{(T - \tau_1^{\text{opt2}})^2}. \quad (53)$$

3) *Communication-Cooperation Mode*: The communication-cooperation mode is feasible only when  $l_{a,\max}^{(2)} \geq L$  with  $l_{a,\max}^{(2)}$  given in (26). With  $l_a = L$  and  $l_u = l_h = 0$ , we have  $P_1 = 0$  and  $\tau_1 = 0$ . Therefore, problem (P2) is re-expressed as

$$\begin{aligned} \min_{\tau_2, \tau_3, P_2, P_3} &\tau_2 P_2 + \tau_3 P_3 \quad (54) \\ \text{s.t. } &L \leq \min(\tau_2 r_0(P_2) + \tau_3 r_1(P_3), \tau_2 r_{01}(P_2)) \\ &\tau_2 + \tau_3 + L c_a / f_{a,\max} \leq T \\ &0 \leq \tau_i \leq T, \forall i \in \{2, 3\} \\ &0 \leq P_2 \leq P_{u,\max}, 0 \leq P_3 \leq P_{h,\max}. \end{aligned}$$

Similarly as for (P1), problem (54) can be optimally solved by Algorithm 1 by setting  $l_u = 0, l_h = 0, l_a = L$ , and  $\tau_1 = 0$ . We denote  $\{\tau_2^{\text{opt2}}, \tau_3^{\text{opt2}}, P_2^{\text{opt2}}, P_3^{\text{opt2}}\}$  as the optimal solution to problem (54). Therefore, we obtain the energy consumption for this mode as

$$E_a^{\text{opt2}} = \tau_2^{\text{opt2}} P_2^{\text{opt2}} + \tau_3^{\text{opt2}} P_3^{\text{opt2}}. \quad (55)$$

4) *Mode Selection*: By comparing  $E_u^{\text{opt2}}$ ,  $E_h^{\text{opt2}}$ , and  $E_a^{\text{opt2}}$ , we determine the computation mode as the one with the minimum energy consumption. Accordingly, the optimal  $l_a, l_u$ , and  $l_h$  are decided, and the corresponding computation and communication resources allocation for that mode becomes the optimal solution to problem (P2). As a result, problem (P2) in the binary offloading case is optimally solved.

## VI. NUMERICAL RESULTS

In this section, numerical results are provided to evaluate the performance of the proposed joint computation and communication cooperation design for both partial and binary offloading cases, as compared to the following benchmark schemes without such a joint design.

- *Local computing*: The user executes the computation tasks locally by itself. The energy consumption for local computing is obtained as  $E_u^{\text{opt2}}$  in (50).
- *Computation cooperation with partial offloading* [24]: The computation tasks are partitioned into two parts for the user's local computing and offloading to the helper, respectively. This corresponds to solving problem (P1) by setting  $l_a = 0$  and  $\tau_2 = \tau_3 = 0$ .
- *Communication cooperation with partial offloading* [10]: The computation tasks are partitioned into two parts for the user's local computing and offloading to the AP, respectively. The offloading is assisted by the helper's communication cooperation as a DF relay. This corresponds to solving problem (P1) by setting  $l_h = 0$  and  $\tau_2 + \tau_3 = T$ .
- *Computation cooperation with binary offloading*: The user offloads all the computation tasks to the helper for remote execution. The energy consumption corresponds to  $E_h^{\text{opt2}}$  in (53).
- *Communication cooperation with binary offloading*: The user can only offload its computation tasks to the AP assisted by the helper's communication cooperation. The energy consumption corresponds to  $E_a^{\text{opt2}}$  in (55) based on (54).

In the simulation, we consider that the user and the AP are located with a distance of 250 meters (m) and the helper is located on the line between them. Let  $D$  denote the distance between the user and the helper. The pathloss between any two nodes is denoted as  $\beta_0 (d/d_0)^{-\zeta}$ , where  $\beta_0 = -60$  dB corresponds to the path loss at the reference distance of  $d_0 = 10$  m,  $d$  denotes the distance from the transmitter to the receiver, and  $\zeta = 3$  is the pathloss exponent. Furthermore, we set  $B = 1$  MHz,  $\sigma_0^2 = \sigma_1^2 = -70$  dBm,  $c_u = c_h = 10^3$  cycles/bit [13],  $\kappa_u = 10^{-27}$  [10],  $\kappa_h = 0.3 \times 10^{-27}$ ,  $P_{u,\max} = P_{h,\max} = 40$  dBm,  $f_{u,\max} = 2$  GHz,  $f_{h,\max} = 3$  GHz, and  $f_{a,\max} = 5$  GHz.

Fig. 3 shows the maximum number of task-input bits versus the block length  $T$ , where  $D = 20$  m. It is observed that for both partial and binary offloading cases under this setup, the computation cooperation and communication cooperation schemes achieve higher computation capacity than the local computing benchmark. Furthermore, for the binary or partial offloading, the communication cooperation scheme is observed

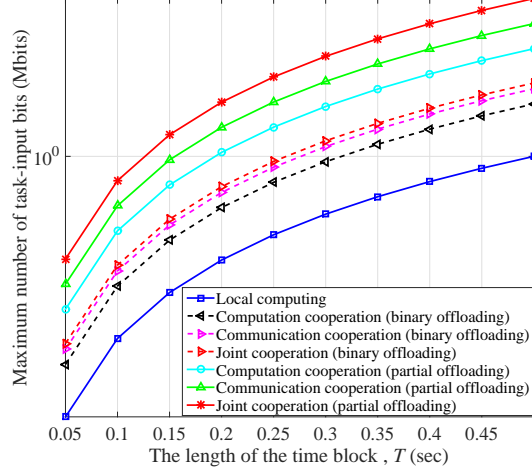


Fig. 3. The maximal number of task-input bits versus the block length.

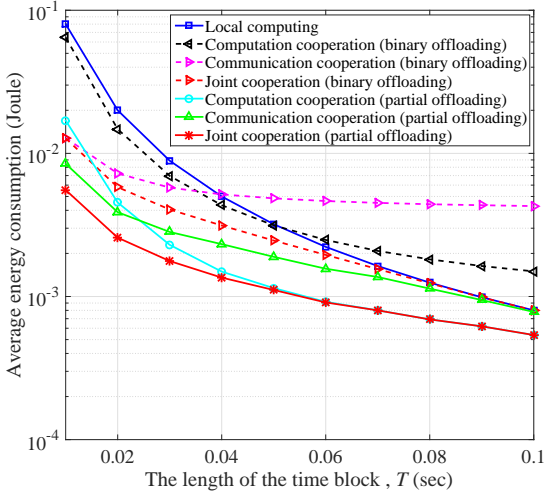


Fig. 4. The average energy consumption versus the block length.

to outperform the corresponding computation cooperation schemes, due to the higher computation capacities at the MEC server. In addition, our proposed joint computation and communication cooperation design is observed to achieve the highest computation capacity by exploiting both benefits.

Fig. 4 shows the average energy consumption versus the block length  $T$ , where  $L = 0.02$  Mbits and  $D = 120$  m. We have the following observations.

- The average energy consumption by all the schemes decreases as  $T$  increases. By comparing the partial and binary offloading, it is observed that the computation and/or communication cooperation approach in the former case achieves more significant energy reduction than the corresponding one in the latter case. This indicates the benefit of task partitions in energy saving for MEC.
- In the binary offloading case, when  $T$  is small (e.g.,  $T < 0.035$  sec), the communication cooperation scheme is observed to achieve the lower energy consumption than the local computing and the computation cooper-

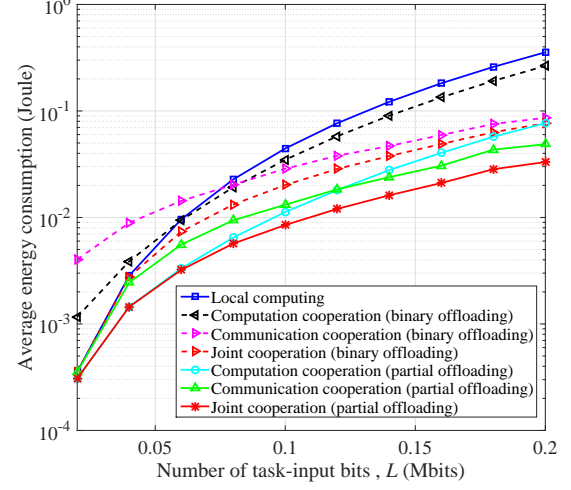


Fig. 5. The average energy consumption versus the number of task-input bits.

ation schemes; when  $0.035$  sec  $< T \leq 0.05$  sec, the computation cooperation scheme outperforms the other two schemes; when  $T$  becomes large (e.g.,  $T > 0.05$  sec), the local computing scheme is beneficial. By exploiting the computation mode selection, the proposed joint cooperation scheme is observed to further reduce the system energy consumption.

- In the partial offloading case, the communication cooperation scheme is observed to achieve lower energy consumption than the computation cooperation scheme when  $T$  is small (e.g.,  $T < 0.025$  sec), while the reverse is true when  $T$  becomes large. It is also observed that the computation cooperation and communication cooperation schemes both outperform the local computing. This is because that the two cooperation schemes additionally exploit computation resources at the helper and the AP, respectively. The proposed joint cooperation scheme is observed to achieve the minimum energy consumption.

Fig. 5 shows the average energy consumption versus the number of task-input bits  $L$ , where  $T = 0.15$  sec and  $D = 120$  m. We have generally similar observations in Fig. 5 as in Fig. 4. Specifically, it is observed that at small  $L$  values (e.g.,  $L < 0.06$  Mbits), the local computing is observed to achieve a similar performance as the proposed joint cooperation scheme with binary offloading, since in this case, the local computing is sufficient to execute the computation task-input bits. As  $L$  increases, the joint computation and communication cooperation is observed to achieve significant performance gain in terms of energy reduction.

Fig. 6 shows the average energy consumption versus  $D$  in both the partial and binary offloading cases, where  $T = 0.3$  sec and  $L = 0.5$  Mbits. It is observed that the average energy consumption by the local computing scheme remains unchanged as  $D$  increases. By contrast, as  $D$  becomes larger, the average energy consumption by the communication cooperation scheme is observed to first decrease and then increase, while that by the computation cooperation scheme is observed to increase monotonically. This is because that as  $D$  increases, the

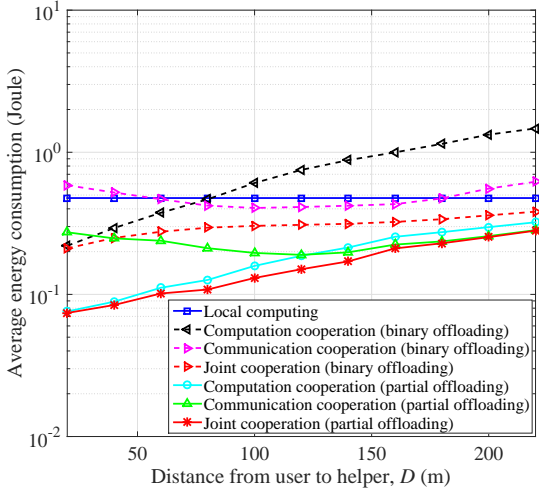


Fig. 6. The average energy consumption versus the distance between the user and the helper.

wireless channel gain between the user and the helper becomes smaller, while that between the helper and the AP becomes stronger; therefore, such a change benefits the offloading from the helper to the AP, but incurs increased offloading energy consumption from the user to the helper. Furthermore, the proposed joint cooperation scheme is observed to achieve significant gains over these benchmark schemes, in terms of energy consumption at all  $D$  values.

## VII. CONCLUSION

In this paper, we proposed a novel joint computation and communication cooperation approach for improving the MEC performance, where nearby helper nodes share the computation and communication resources to help actively-computing user nodes. By considering a basic three-node model under a four-slot cooperation protocol, we developed an energy-efficient design framework for both partial and binary offloading cases. We minimized the total energy consumption at both the user and the helper subject to the computation latency constraint, by jointly optimizing the task partition, as well as the computation and communication resources allocation. Based on convex optimization techniques, an efficient algorithm had been presented to obtain the optimal solution in the partial offloading case. Computation mode selection was then applied for optimally solving the problem in the binary offloading case. Extensive numerical results demonstrated the merit of the proposed joint computation and communication cooperation scheme over alternative benchmarks. It is our hope that this paper sheds new light on how to optimally design multi-resource user cooperation to improve the operation efficiency of MEC.

## APPENDIX

### A. Proof of Lemma 4.1

Note that for  $\mathcal{L}(\mathbf{E}, \boldsymbol{\tau}, \mathbf{l}, \boldsymbol{\lambda}, \boldsymbol{\mu})$  in (29), there exist two terms  $(\lambda_1 - \mu_2)l_h$  and  $(\lambda_2 + \lambda_3 + \mu_1 c_a/f_{a,\max} - \mu_2)l_a$ . Suppose

$\lambda_1 - \mu_2 < 0$  (or  $\lambda_2 + \lambda_3 + \mu_1 c_a/f_{a,\max} - \mu_2 < 0$ ). Then  $\mathcal{L}(\mathbf{E}, \boldsymbol{\tau}, \mathbf{l}, \boldsymbol{\lambda}, \boldsymbol{\mu})$  becomes negative infinity when  $l_h \rightarrow +\infty$  (or  $l_a \rightarrow +\infty$ ). This implies that the dual function  $g(\boldsymbol{\lambda}, \boldsymbol{\mu})$  is unbounded from below in this case. Hence, it requires that  $\lambda_1 - \mu_2 \geq 0$  and  $\lambda_2 + \lambda_3 + \mu_1 c_a/f_{a,\max} - \mu_2 \geq 0$  to guarantee  $g(\boldsymbol{\lambda}, \boldsymbol{\mu})$  to be bounded from below. Lemma 4.1 thus follows.

### B. Proof of Lemma 4.2

As problem (31) is convex and satisfies the Slater's condition, strong duality holds between problem (31) and its dual problem. Therefore, one can solve this problem by applying the KKT conditions [29]. The Lagrangian of problem (31) is given by

$$\begin{aligned} \mathcal{L}_1 = & E_1 + \mu_1 \tau_1 - \lambda_1 \tau_1 r_{01} \left( \frac{E_1}{\tau_1} \right) - \mu_2 l_h + \lambda_1 l_h + \frac{\kappa_h c_h^3 l_h^3}{(T - \tau_1)^2} \\ & - a_1 E_1 + \alpha_1 (E_1 - \tau_1 P_{u,\max}) - b_1 \tau_1 + b_2 (\tau_1 - T) \\ & - d_1 l_h + \beta_1 \left( l_h - \frac{(T - \tau_1) f_{h,\max}}{c_h} \right), \end{aligned}$$

where  $a_1, \alpha_1, b_1, b_2, d_1$ , and  $\beta_1$  are the non-negative Lagrange multipliers associated with  $E_1 \geq 0$ ,  $E_1 \leq \tau_1 P_{u,\max}$ ,  $\tau_1 \geq 0$ ,  $\tau_1 \leq T$ ,  $l_h \geq 0$ , and  $l_h \leq (T - \tau_1) f_{h,\max} / c_h$ , respectively.

Based on the KKT conditions, it follows that

$$a_1 E_1 = 0, \quad \alpha_1 (E_1 - \tau_1 P_{u,\max}) = 0, \quad b_2 (\tau_1 - T) = 0 \quad (56a)$$

$$b_1 \tau_1 = 0, \quad d_1 l_h = 0, \quad \beta_1 \left( l_h - \frac{(T - \tau_1) f_{h,\max}}{c_h} \right) = 0 \quad (56b)$$

$$\frac{\partial \mathcal{L}_1}{\partial E_1} = 1 - \frac{\lambda_1 B \frac{h_{01}}{\sigma_1^2}}{\ln 2 \left( 1 + \frac{E_1 h_{01}}{\tau_1 \sigma_1^2} \right)} - a_1 + \alpha_1 = 0 \quad (56c)$$

$$\begin{aligned} \frac{\partial \mathcal{L}_1}{\partial \tau_1} = & \frac{2 \kappa_h c_h^3 l_h^3}{(T - \tau_1)^3} - \lambda_1 B \log_2 \left( 1 + \frac{E_1 h_{01}}{\tau_1 \sigma_1^2} \right) + \frac{\beta_1 f_{h,\max}}{c_h} \\ & + \mu_1 + \frac{\lambda_1 B \frac{h_{01}}{\sigma_1^2} \frac{E_1}{\tau_1}}{\ln 2 \left( 1 + \frac{E_1 h_{01}}{\tau_1 \sigma_1^2} \right)} - b_1 + b_2 + \alpha_1 P_{u,\max} = 0 \end{aligned} \quad (56d)$$

$$\frac{\partial \mathcal{L}_1}{\partial l_h} = \frac{3 \kappa_h c_h^3 l_h^2}{(T - \tau_1)^2} - \mu_2 + \lambda_1 - d_1 + \beta_1 = 0, \quad (56e)$$

where (56a) and (56b) denote the complementary slackness condition, (56c), (56d) and (56e) are the first-order derivative conditions of  $\mathcal{L}_1$  with respect to  $E_1$ ,  $\tau_1$ , and  $l_h$ , respectively. Therefore, we have (36) based on (56c), and (37) holds due to (56e). Furthermore, based on (56c), (56d), and (56e) and with some manipulations, we have (41) and (42).

Furthermore, by substituting (36) and (37) into (56d) and assuming  $\rho_1 = b_2 - b_1$ , we have  $\rho_1$  in (40). Hence, the optimal  $\tau_1^*$  is given in (38). This lemma is thus proved.

## REFERENCES

- [1] X. Cao, F. Wang, J. Xu, R. Zhang, and S. Cui, "Joint computation and communication cooperation for mobile edge computing," in *Proc. WiOpt Workshops-EFC-IoT*, Shanghai, China, May 2018, pp. 1–5.
- [2] M. Chiang and T. Zhang, "Fog and IoT: An overview of research opportunities," *IEEE Internet Thing J.*, vol. 3, no. 6, pp. 854–864, Jun. 2016.

[3] H. Dinh, C. Lee, D. Niyato, and P. Wang, "A survey of mobile cloud computing: Architecture, applications, and approaches," *Wirel. Commun. Mob. Comput.*, vol. 13, no. 18, pp. 1587–1611, Dec. 2013.

[4] ETSI White Paper, "Mobile-edge computing: A key technology towards 5G," 2015. [Online]. Available: [http://www.etsi.org/images/files/ETSIWhitePapers/etsi\\_wP11\\_mec\\_a\\_key\\_technology\\_towards\\_5g.pdf](http://www.etsi.org/images/files/ETSIWhitePapers/etsi_wP11_mec_a_key_technology_towards_5g.pdf)

[5] P. Mach and Z. Becvar, "Mobile edge computing: A survey on architecture and computation offloading," *IEEE Commun. Surveys Tuts.*, vol. 19, no. 3, pp. 1628–1656, 3rd Quart., 2017.

[6] Y. Mao, C. You, J. Zhang, K. Huang, and K. B. Letaief, "A survey on mobile edge computing: The communication perspective," *IEEE Commun. Surveys Tuts.*, vol. 19, no. 4, pp. 2322–2358, 4th Quart., 2017.

[7] S. Barbarossa, S. Sardellitti, and P. D. Lorenzo, "Communicating while computing: Distributed mobile cloud computing over 5G heterogeneous networks," *IEEE Signal Process. Mag.*, vol. 31, no. 6, pp. 45–55, Nov. 2014.

[8] J. Liu, Y. Mao, J. Zhang, and K. B. Letaief, "Delay-optimal computation task scheduling for mobile-edge computing systems," in *Proc. IEEE ISIT*, Spain, Jun. 2016, pp. 1451–1455.

[9] Y. Zhang, D. Niyato, and P. Wang, "Offloading in mobile cloudlet systems with intermittent connectivity," *IEEE Trans. Mobile Comput.*, vol. 14, no. 12, pp. 2516–2529, Dec. 2015.

[10] C. You, K. Huang, H. Chae, and B. Kim, "Energy-efficient resource allocation for mobile-edge computing offloading," *IEEE Trans. Wireless Commun.*, vol. 16, no. 3, pp. 1397–1411, Mar. 2017.

[11] F. Wang, J. Xu, and Z. Ding, "Optimized multiuser computation offloading with multi-antenna NOMA," in *Proc. IEEE GLOBECOM Workshops-NOMAT5G*, Singapore, Dec. 2017, pp. 1–7.

[12] M.-H. Chen, M. Dong, and B. Liang, "Joint offloading decision and resource allocation for mobile cloud with computing access point," in *Proc. IEEE ICASSP*, Shanghai, China, Mar. 2016, pp. 3516–3520.

[13] F. Wang, J. Xu, X. Wang, and S. Cui, "Joint offloading and computing optimization in wireless powered mobile-edge computing system," *IEEE Trans. Wireless Commun.*, vol. 17, no. 3, pp. 1784–1797, Mar. 2018.

[14] C. You, K. Huang, and H. Chae, "Energy efficient mobile cloud computing powered by wireless energy transfer," *IEEE J. Sel. Areas Commun.*, vol. 34, no. 5, pp. 1757–1770, May 2016.

[15] S. Bi and Y. J. Zhang, "Computation rate maximization for wireless powered mobile-edge computing with binary computation offloading," to appear in *IEEE Trans. Wireless Commun.*, 2018. [Online]. Available: <https://arxiv.org/abs/1708.08810>

[16] A. Nosratinia and A. Hedayat, "Cooperative communication in wireless networks," *IEEE Commun. Mag.*, vol. 42, no. 10, pp. 74–80, Oct. 2004.

[17] A. Sendonaris, E. Erkip, and B. Aazhang, "User cooperation diversity: Part I. system description," *IEEE Trans. Commun.*, vol. 51, no. 11, pp. 1927–1938, Nov. 2003.

[18] J. N. Laneman, D. Tse, and G. W. Wornell, "Cooperative diversity in wireless networks: Efficient protocols and outage behavior," *IEEE Trans. Inform. Theory*, vol. 50, no. 11, pp. 3062–3080, Nov. 2004.

[19] Y. Liang and V. V. Veeravalli, "Gaussian orthogonal relay channels: Optimal resource allocation and capacity," *IEEE Trans. Inform. Theory*, vol. 51, no. 9, pp. 3284–3289, Sep. 2005.

[20] H. Ju and R. Zhang, "User cooperation in wireless powered communication networks," in *Proc. IEEE GLOBECOM*, Austin, TX, USA, Dec. 2014, pp. 1430–1435.

[21] X. Hu, K. K. Wong, and K. Yang, "Wireless powered cooperation-assisted mobile edge computing," *IEEE Trans. Wireless Commun.*, vol. 17, no. 4, pp. 2375–2388, Apr. 2018.

[22] M. Xiao, J. Wu, L. Huang, Y. Wang, and C. Liu, "Multi-task assignment for crowdsensing in mobile social networks," in *Proc. IEEE INFOCOM*, Kowloon, Apr./May 2015, pp. 2227–2235.

[23] Z. Sheng, C. Mahapatra, V. C. M. Leung, M. Chen, and P. K. Sahu, "Energy efficient cooperative computing in mobile wireless sensor networks," *IEEE Trans. Cloud Comput.*, vol. 6, no. 1, pp. 114–126, 1st Quart., 2018.

[24] L. Pu, X. Chen, J. Xu, and X. Fu, "D2D fogging: An energy-efficient and incentive-aware task offloading framework via network-assisted D2D collaboration," *IEEE J. Sel. Areas Commun.*, vol. 34, no. 12, pp. 3887–3901, Nov. 2016.

[25] C. You and K. Huang, "Exploiting non-causal CPU-state information for energy-efficient mobile cooperative computing," to appear in *IEEE Trans. Wireless Commun.*, 2018. [Online]. Available: <https://arxiv.org/abs/1704.04595>

[26] T. D. Burd and R. W. Brodersen, "Processor design for portable systems," *Kluwer J. VLSI Signal Process. Syst.*, vol. 13, no. 2/3, pp. 203–221, Aug. 1996.

[27] A. Ruszczyski, *Nonlinear Optimization*, Princeton Univ. Press, Princeton, NJ, 2006.

[28] S. Boyd, "Ellipsoid method," Stanford Univ., California, USA. [Online]. Available: [https://web.stanford.edu/class/ee364b/lectures/ellipsoid\\_method\\_slides.pdf](https://web.stanford.edu/class/ee364b/lectures/ellipsoid_method_slides.pdf)

[29] S. Boyd and L. Vandenberghe, *Convex Optimization*, Cambridge, U.K.: Cambridge Univ. Press, Mar. 2004.